Ind. J. Pharm. Edu. Res, 2023; 57(1s):s105-s113.
https://www.ijper.org

Original Article

Analog-based Design and Development of Novel Molecules as Anti-tubercular Agents

Satheeshkumar Sellamuthu[1,*], Mohan Sellapan[1], Kandasamy CS[1], Dileep Kumar[2, 3, 4], Kavitha Kasimayan[1], Sasikala Manickavasagam[1]

[1]Karpagam College of Pharmacy, Othakkalmandapam, Coimbatore, Tamil Nadu, INDIA.
[2]Poona College of Pharmacy, Bharati Vidyapeeth (Deemed to be University), Pune Maharashtra, INDIA.
[3]Department of Entomology, University of California, Davis, One Shields Ave, Davis, CA, USA.
[4]UC Davis Comprehensive Cancer Centre, University of California, Davis, One Shields Ave, Davis, CA, USA.

ABSTRACT

Background: The burden of *tuberculosis* is immense as most of the drugs developed resistance to *Mycobacterium tuberculosis* (Mtb). This issue shall be addressed by developing new drugs acting through novel mechanisms. GSK 2556286 (GSK-286) is a phase 1 clinical candidate with a novel mechanism of action related to cholesterol catabolism, hence it was selected as template/ parent molecules for our analogue-based drug design strategy. **Materials and Methods:** The novel-designed molecules were initially checked to be drug-like using 'Lipinski's rule of five and synthesized with good yields. The obtained compounds were evaluated for anti-tubercular activity against Mtb *H37Rv,* antibacterial activity against *S. aureus* and *E. coli*, cytotoxicity screening against mammalian VERO cells and BBB permeability against Porcine Brain Lipid. Docking was also performed against HsaA monooxygenase (PDB ID: 3AFF) to understand the possible mechanism of action. **Results and Conclusion:** The compounds 3a and 7a exhibited promising anti-tubercular activity at MIC of 3.13 µg/mL. Further, the compounds proved to be effective towards *S. aureus* at 0.98 µg/mL and *E. coli* at 7.81 µg/mL. The molecules 3a and 7a produced good docking scores of -9.2 and -9.3 kcal/mole respectively. The association between docking results and anti-tubercular activity has postulated that the molecules could act through novel mechanisms by inhibiting HsaA monooxygenase. Moreover, all the compounds in the study produced very less cytotoxicity at CC_{50} > 190 µg/mL against mammalian VERO cells and also showed minimal BBB permeability in PAMPA assay. The effective anti-tubercular activity of the lead molecules with additional safety against mammalian VERO cells with reduced BBB permeability could provide a new standpoint in anti-tubercular drug discovery.

Keywords: Analog-based Design, Anti-tubercular activity, BBB permeability, GSK 2556286, VERO cells.

Correspondence:
Dr. Satheeshkumar Sellamuthu
Associate Professor, Karpagam College of Pharmacy, Othakkalmandapam, Coimbatore-641032, Tamil Nadu, INDIA.
Email id: satheeshpharma6@gmail.com

Received: 10-10-2022;
Revised: 08-12-2022;
Accepted: 03-01-2023.

INTRODUCTION

Tuberculosis (TB) was the foremost cause of death until the emergence of COVID-19 due to a single infectious agent.[1] The challenges in controlling TB were attributed to the rapid development of resistant strains and comorbidity of HIV along with TB.[2] WHO estimated that 10 million people get affected by TB in 2020. Among them, men accounted for 5.6 million cases, women 3.3 million and children 1.1 million cases.[3] An effective method to control any infectious disease is vaccination.[4] The BCG vaccine is used as a preventive measure in the control of TB, but *Mycobacterium tuberculosis* (Mtb) masks the protective efficacy of the vaccine by inducing heterologous immunity.[5,6] The severe cases of drug-resistant TB viz. MDR-TB and XDR-TB are reported which pose a serious threat to the control of TB. Hence, new treatments are the need of the hour to combat the deadly infectious disease. Several drug candidates are in the pipeline with efforts on developing new drugs for treating TB. After the approval of Rifapentine in 1998 to treat TB, Bedaquiline, Pretomanid and Delamanid were the only three new drugs that got US-FDA approval in recent years.[7,8] Therefore, there is a huge necessity for the discovery of novel mechanism-acting TB drugs to battle the different resistant strains of TB. GlaxoSmithKline, Melinda Gates Foundation and TB Drug Accelerator groups are working together on the development of GSK2556286 as a novel drug with a new mechanism of action in treating TB. GSK2556286 acts by inhibiting a novel enzyme target, HsaA monooxygenase involved in cholesterol metabolism.[9] The objective of this study is to develop lead molecules homologous to GSK2556286, a phase 1 clinical candidate and acting through the novel target HsaA monooxygenase. The approach of drug design is to retain and

DOI: 10.5530/ijper.57.1s.12

modify certain parts of pharmacophore and linker in an attempt to attain novel molecules analogues to GSK2556286. Thereby, the designed molecules could act through a novel mechanism of action by inhibiting cholesterol metabolism. During the design of molecules, we retained the phenoxy group from GSK2556286, modified the piperidine to benzene and uracil to a substituted-phenyl ring from GSK2556286 to obtain a series of novel molecules (Figure 1) and the novelty of these molecules was affirmed through ZINC database search with all subsets. The molecules were further checked against Lipinski's rule of five to affirm the drug-likeness and later taken for synthesis and biological evaluation for antitubercular activity, antibacterial activity, cytotoxicity and BBB permeability.

MATERIALS AND METHODS

Procedure for Synthesis of 1-bromo-4-phenoxybenzene (2)

Diphenyl ether (1.7g, 0.01M) was dissolved in carbon tetrachloride (100 mL) and bromine solution (1.6g, 0.02M) was added slowly with occasional stirring for 1 hr. Hydrogen bromide evolved during the reaction. The solvent was distilled to obtain the crude product. The byproducts viz dibromo diphenyl ether and other higher brominated derivatives were removed in petroleum ether.[10]

Procedure for the Synthesis of 1-(4-phenoxyphenyl) urea (3)

1-bromo-4-phenoxybenzene (2.5g, 0.01M) and urea (1.2g, 0.02M) were dissolved in Dichloromethane (DCM). Then, 1mL (0.01M) of triethylamine was added and refluxed for 2 hr.[11] The solvent in the reaction mixture was removed through distillation. The residue obtained was purified through an acid-base workup to get pure 1-(4-phenoxyphenyl)urea.[11]

Procedure involved in the Synthesis of diphenyl ether tethered urea derivatives (1a-15a)

1-(4-phenoxyphenyl)urea (3) (2.3g, 0.01M), obtained in the previous step appropriate was added with corresponding chloro-benzenes (0.02M), K_2CO_3 (0.005M) and KI (0.05M) and refluxed using THF as a solvent for 3 hr at 80°C.[12] The progression of the chemical reaction was checked by performing TLC. After the completion of the reaction, the crude reaction mixture was transferred into crushed ice with stirring. Precipitates of different diphenylether-tethered urea derivatives were obtained, then filtered and washed with a brine solution and water. Further on the requirement, impure products were introduced in column chromatography using SiO_2 as the stationary phase and ethyl acetate: hexane as the mobile phase at different ratios (Figure 2).

1-(4-phenoxyphenyl)-3-phenylurea (1a)

Yield: 84%; MP: 143-146°C; IR (KBr, cm^{-1}): 3427 (N-H Stretch), 3097 (=CH Stretch), 1742 (C=O Stretch), 1606 (C=C Stretch); 500 MHz- ^{1}H-NMR, Solvent-$CDCl_3$ δ (ppm); 7.395-7.259 (m, 9H, Biphenyl-CH)); 7.224-7.208 (t, 2H, J=8, C3, C5-phenyl), 7.125-7.110 (t, 2H, J=7.5, C2, C6-phenyl), 7.096-7.080 (t, 1H, J=8, C4-phenyl), 3.954 (s, 1H, NH) 3.828 (s, 1H, NH); 125 MHz- ^{13}C-NMR, Solvent-$CDCl_3$ δ: 167.323 (C=O), 142.012, 141.884, 130.624, 130.108, 129.337, 128.670, 127.215, 126.843, 126.197 (Aromatic carbons), ESI-MASS (*m/z*): calculated-304.35, found-305.5 (M+1, 45.2%).

1-(4-nitrophenyl)-3-(4-phenoxyphenyl)urea (2a)

Yield: 79%; MP: 154-156°C; IR (KBr, cm^{-1}): 3422 (N-H Stretch), 3105 (=CH Stretch), 1746 (C=O Stretch), 1606 (C=C Stretch), 1543 (NO_2 asymmetric stretch); 500 MHz- ^{1}H-NMR, Solvent-$CDCl_3$ δ (ppm); 7.381-7.293 (m, 9H, Biphenyl-CH), 7.058-7.044, (dd, J=9, 1.5 Hz, 2H, C3-phenyl, C5-phenyl), 6.714, 6.697 ((dd, J=8.0, 1.5 Hz, 2H, C2-phenyl, C6-phenyl), 4.004 (s, 1H, NH) 3.894 (s, 1H, NH); 125 MHz- ^{13}C-NMR, Solvent-$CDCl_3$ δ: 166.312 (C=O), 143.084, 141.952, 129.991, 129.683, 129.472, 129.235, 128.857, 128.639, 128.274, 127.715, 126.763, 126.266, 125.778, 119.333, 119.165, 119.028, 116.002 (Aromatic carbons), ESI-MASS (*m/z*): calculated-349.35, found- 350.7 (M+1, 74%).

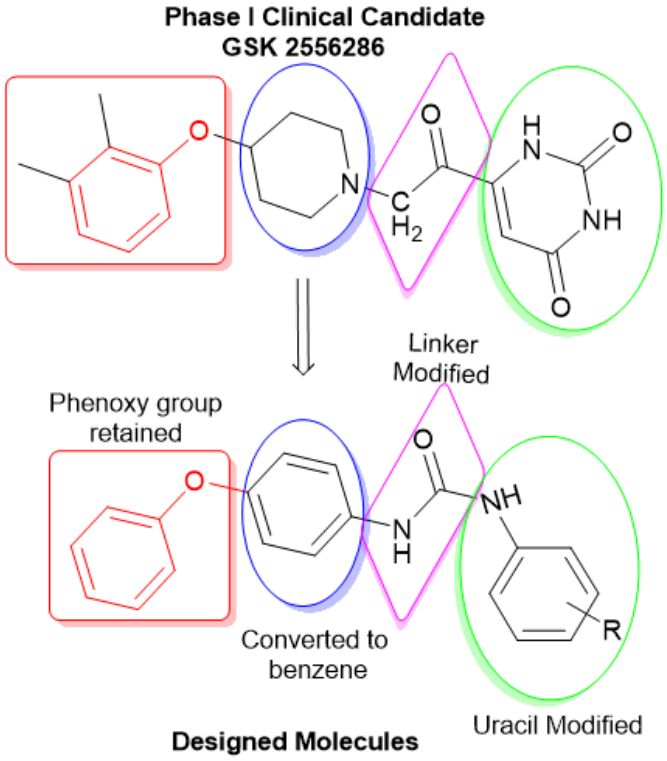

Figure 1: Strategy used in the design of new molecules.

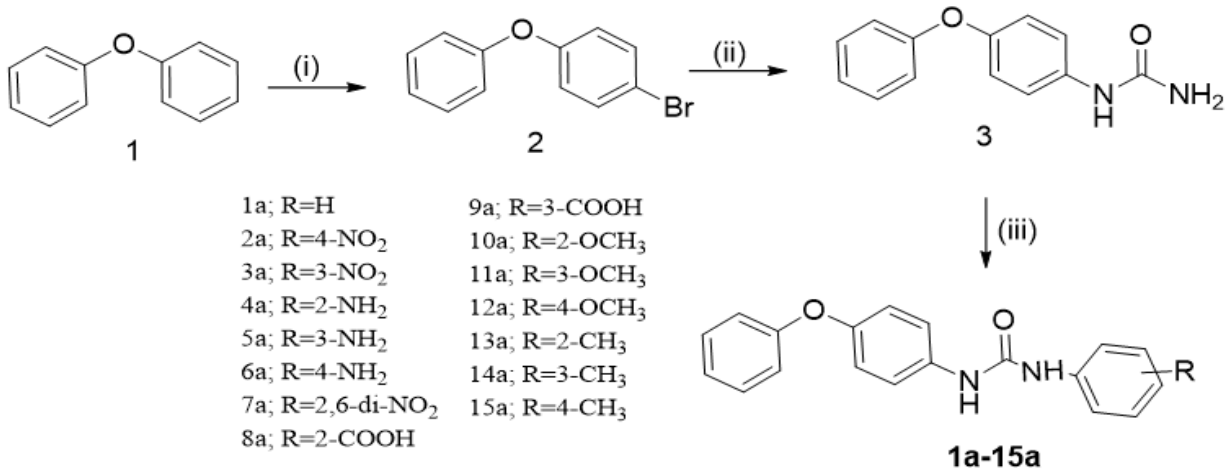

Figure 2: Synthetic scheme of the designed molecules.

1-(3-nitrophenyl)-3-(4-phenoxyphenyl)urea (3a)

Yield: 75%; MP: 153-155°C; IR (KBr, cm^{-1}): 3425 (N-H Stretch), 3089 (=CH Stretch), 1747 (C=O Stretch), 1604 (C=C Stretch), 1536 (NO_2 asymmetric stretch); 500 MHz- ^{1}H-NMR, Solvent-$CDCl_3$ δ (ppm); 7.377-7.290 (m, 9H, Biphenyl-CH), 7.253-7.220 (t, 1H, J=7, C5-phenyl), 7.153-7.140 (d, 1H, J=8.5, C4-phenyl), 6.872-6.822 (m, 2H, C4, C6-phenyl) 3.991 (s, 1H, NH), 3.892 (s, 1H, NH); 125 MHz- ^{13}C-NMR, Solvent-$CDCl_3$ δ: 166.308 (C=O), 143.079, 141.946, 129.986, 129.679, 129.468, 129.228, 128.854, 128.633, 128.268, 127.711, 126.761, 126.262, 125.772, 119.332, 119.159, 119.025, 115.991 (Aromatic carbons); ESI-MASS (*m/z*): calculated-349.35, found- 350.7 (M+1, 74%).

1-(2-aminophenyl)-3-(4-phenoxyphenyl)urea (4a)

Yield: 70%; MP: 145-148°C; IR (KBr, cm^{-1}): 3460, 3412 (NH_2 Stretch), 3094 (=CH Stretch), 1753 (C=O Stretch), 1608 (C=C Stretch); 500 MHz- ^{1}H-NMR, Solvent-$CDCl_3$ δ (ppm); 7.383-7.248 (m, 9H, Biphenyl-CH), 7.091-7.068 (t, 1H, J=7, C5-phenyl), 6.816-6.887 (d, 1H, J=8.5, C4-phenyl), 6.605-6.576 (m, 2H, C4-phenyl, C6-phenyl), 3.925 (s, 1H, NH) 3.868 (s, 1H, NH) 3.397 (2H, NH_2); 125 MHz- ^{13}C-NMR, Solvent-$CDCl_3$ δ: 166.289 (C=O), 145.018, 141.889, 141.668, 130.999, 130.236, 130.025, 129.727, 129.410, 129.190, 128.575, 128.364, 128.115, 126.819, 126.579, 126.291, 126.003, 123.248, 116.337 (Aromatic carbons), ESI-MASS (*m/z*): calculated-319.36, found- 320.8 (M+1, 75%).

1-(3-aminophenyl)-3-(4-phenoxyphenyl)urea (5a)

Yield: 69%; MP: 148-150°C, IR (KBr, cm^{-1}): 3508, 3455 (NH_2 Stretch), 3095 (=CH Stretch), 1743 (C=O Stretch), 1601 (C=C Stretch); 500 MHz- ^{1}H-NMR, Solvent-$CDCl_3$ δ (ppm); 7.384-7.296 (m, 9H, Biphenyl-CH), 7.052-7.038, (t, 1H, J=7, C5-phenyl), 6.710, 6.693 (d, 1H, J=8.5, C4-phenyl), 6.559-6.508 (m, 2H, C2-phenyl, C6-phenyl), 4.081 (s, 1H, NH), 4.906 (s, 1H, NH), 3.293 (s, 2H, NH_2); 125 MHz- ^{13}C-NMR, Solvent-$CDCl_3$ δ: 166.298 (C=O), 147.725, 141.937, 134.910, 130.370, 130.063, 129.689, 129.410, 129.199, 128.700, 128.124, 126.809, 126.300, 126.070, 125.859, 125.542, 118.506, 115.051, 113.323 (Aromatic carbons); ESI-MASS (*m/z*): calculated-319.36, found- 320.5 (M+1, 72%).

1-(4-aminophenyl)-3-(4-phenoxyphenyl)urea (6a)

Yield: 66%; MP: 152-155°C; IR (KBr, cm^{-1}): 3502, 3448 (NH_2 Stretch), 3089 (=CH Stretch), 1739 (C=O Stretch), 1600 (C=C Stretch); 500 MHz- ^{1}H-NMR, Solvent-$CDCl_3$ δ (ppm); 7.384, 7.308 (m, 9H, Biphenyl-CH), 7.250, 7.235 (d, 2H, J=7.5, C3-phenyl, C5-phenyl), 6.855, 6.838 (d, 2H, J=8.5, C2, C6-phenyl), 3.982 (s, 1H, NH), 3.802 (s, 1H, NH), 3.173 (s, 2H, NH_2); 125 MHz-125 MHz- ^{13}C-NMR, Solvent-$CDCl_3$ δ: 166.289 (C=O), 143.770, 142.455, 141.908, 130.102, 129.785, 129.401, 129.055, 128.700, 126.560, 126.195, 125.792, 116.164, 115.799, 115.627, 113.985, 113.928 (Aromatic carbons); ESI-MASS (*m/z*): calculated-319.36, found- 320.3 (M+1, 74%).

1-(2,6-dinitrophenyl)-3-(4-phenoxyphenyl)urea (7a)

Yield: 75%; MP: 160-162°C, IR (KBr, cm^{-1}): 3431 (N-H Stretch), 3091 (=CH Stretch), 1748 (C=O Stretch), 1614 (C=C Stretch), 1549 (NO_2 asymmetric stretch); 500 MHz- ^{1}H-NMR, Solvent-$CDCl_3$ δ (ppm): 7.384, 7.296 (m, 9H, Biphenyl-CH), 7.048-7.034, (d, 2H, J=7, C3-phenyl and C5-phenyl), 6.811, 6.794 (m, 1H, C4-phenyl), 3.999 (s, 1H, NH), 3.864 (s, 1H, NH); 125 MHz- ^{13}C-NMR, Solvent-$CDCl_3$ δ: 166.298 (C=O), 147.926, 141.937, 130.658, 130.543, 130.044, 129.766, 129.410, 128.959, 128.585, 128.115, 127.040, 126.665, 126.195, 125.734, 123.104,

121.386, 117.921, 113.736 (Aromatic carbons); ESI-MASS (*m/z*): calculated-394.34, found- 395.4 (M+1, 70%).

2-(3-(4-phenoxyphenyl)ureido)benzoic acid (8a)

Yield: 60%; MP: 158-160°C, IR (KBr, cm^{-1}): 3456 (O-H Stretch), 3228 (N-H Stretch), 3096 (=CH Stretch), 1737 (C=O Stretch-carbamide), 1694 (C=O Stretch-carboxylic), 1599 (C=C Stretch); 500 MHz- ^{1}H-NMR, Solvent-$CDCl_3$ δ (ppm): 12.203 (s, 1H, OH), 7.814, 7.798 (d, J=8 Hz, 1H, C3-phenyl), 7.389-7.308 (m, 9H, Biphenyl-CH), 7.013, 6.988 (m, 2H, C4-phenyl, C6-phenyl, 6.794-6.768 (t, J=7 Hz, 1H, C5-phenyl), 3.551 (s, 1H, NH) 3.411 (s, 1H, NH); 125 MHz- ^{13}C-NMR, Solvent-$CDCl_3$ δ: 166.289 (C=O), 145.546, 141.937, 132.079, 130.159, 129.977, 129.785, 129.410, 129.209, 128.662, 128.537, 128.297, 127.942, 127.385, 126.636, 126.291, 126.108, 125.888, 116.798, 110.242 (Aromatic carbons); ESI-MASS (*m/z*): calculated-348.36, found-349.8 (M+1, 70%).

3-(3-(4-phenoxyphenyl)ureido)benzoic acid (9a)

Yield: 62%; MP: 162-165°C, IR (KBr, cm^{-1}): 3461 (O-H Stretch), 3235 (N-H Stretch), 3089 (=CH Stretch), 1758 (C=O Stretch-carbamide), 1710 (C=O Stretch-carboxylic), 1599 (C=C Stretch); 500 MHz- ^{1}H-NMR, Solvent-$CDCl_3$ δ (ppm): 12.218 (s, 1H, OH), 7.535-7.498 (m, 2H, C2, C4-phenyl) 7.392-7.258 (m, 9H, Biphenyl-CH), 7.112-7.098 (t, J=7.5 Hz, 1H, C5-phenyl), 7.003-6.892 (d, 1H, C6-phenyl), 3.524 (s, 1H, NH); 3.434 (s, 1H, NH); 125 MHz- ^{13}C-NMR, Solvent-$CDCl_3$ δ: 166.289 (C=O), 148.329, 142.157, 141.927, 135.477, 130.236, 129.977, 129.410, 128.969, 128.220, 128.009, 127.855, 127.510, 126.876, 126.233, 125.830, 118.372, 113.294 (Aromatic carbons); ESI-MASS (*m/z*): calculated- 348.36, found- 349.8 (M+1, 75%).

1-(2-methoxyphenyl)-3-(4-phenoxyphenyl)urea (10a)

Yield: 68%; MP: 170-172°C, IR (KBr, cm^{-1}): 3436 (N-H Stretch), 3087 (=C-H Stretch), 2923 (-C-H Stretch), 1755 (C=O Stretch-carbamide), 1607 (C=C Stretch), 1220 (C-O Stretch); 500 MHz- ^{1}H-NMR, Solvent-$CDCl_3$ δ (ppm): 7.392-7.301 (m, 9H, Biphenyl-CH), 7.375-7.256 (m, 3H, C3, C4, C6-phenyl) 6.989 (t, 1H, C5-phenyl), 3.538 (s, 1H, NH), 3.691 (s, 1H, NH), 3.291 (s, 3H, CH_3); 125 MHz- ^{13}C-NMR, Solvent-$CDCl_3$ δ: 166.289 (C=O), 148.771, 141.927, 141.860, 130.015, 129.823, 129.458, 129.055, 128.710, 128.355, 128.057, 126.963, 126.694, 126.243, 126.003, 125.619, 123.709, 123.402, 116.587 (Aromatic carbons), 32.725 (methyl carbon); ESI-MASS (*m/z*): calculated- 334.38, found- 335.4 (M+1, 70%).

1-(3-methoxyphenyl)-3-(4-phenoxyphenyl)urea (11a)

Yield: 65%; MP: 168-170°C; IR (KBr, cm^{-1}): 3433 (N-H Stretch), 3086 (=C-H Stretch), 2941 (-C-H Stretch), 1746 (C=O Stretch-carbamide), 1606 (C=C Stretch), 1158 (C-O Stretch); 500 MHz- ^{1}H-NMR, Solvent-$CDCl_3$ δ (ppm); 7.394-7.258 (m, 9H, Biphenyl-CH), 7.252-7.188, (t, 1H, J=8, C5-phenyl), 6.846, 6.789 (d, 1H, J=8.0, C6-phenyl), 6.648-6.507 (m, 2H, C2, C4-phenyl), 3.328 (s, 1H, NH), 3.198 (s, 3H, CH_3); 125 MHz- ^{13}C-NMR, Solvent-$CDCl_3$ δ: 166.289 (C=O), 152.649, 150.748, 143.204, 141.908, 130.169, 129.257, 128.595, 128.259, 126.761, 126.204, 125.926, 121.117, 120.973, 116.999, 116.827, 116.491, 114.312 (Aromatic carbons), 38.165 (methyl carbon); ESI-MASS (*m/z*): calculated- 334.38, found- 335.9 (M+1, 70%).

1-(4-methoxyphenyl)-3-(4-phenoxyphenyl)urea (12a)

Yield: 64%; MP: 172-174°C, IR (KBr, cm^{-1}): 3427 (N-H Stretch), 3079 (=C-H Stretch), 2950 (-C-H Stretch), 1738 (C=O Stretch-carbamide), 1586 (C=C Stretch), 1162 (C-O Stretch); 500 MHz- ^{1}H-NMR, Solvent-$CDCl_3$ δ (ppm): 7.391-7.256 (m, 9H, Biphenyl-CH), 7.157-7.036 (dd, J=9, 1.4 Hz, 2H, C3-phenyl, C5-phenyl), 6.925, 6.917 (dd, J=8, 1.5 Hz, 2H, C2, C6-phenyl), 3.671 (s, 1H, NH), 3.546 (s, 1H, NH), 3.154 (s, 3H, CH_3); 125 MHz- ^{13}C-NMR, Solvent-$CDCl_3$ δ: 166.289 (C=O), 141.917, 141.754, 130.505, 130.082, 129.506, 129.410, 128.930, 128.575, 128.335, 127.155, 126.876, 126.550, 126.070, 125.696, 119.389, 119.188, 116.107, 115.416, 115.233 (Aromatic carbons), 38.744 (methyl carbon); ESI-MASS (*m/z*): calculated- 334.38, found- 335.7 (M+1, 70%).

1-(4-phenoxyphenyl)-3-(o-tolyl)urea (13a)

Yield: 70%; MP: 151-152°C, IR (KBr, cm^{-1}): 3425 (N-H Stretch), 3095 (=C-H Stretch), 2975 (-C-H Stretch), 1746 (C=O Stretch-carbamide), 1603 (C=C Stretch); 500 MHz- ^{1}H-NMR, Solvent-$CDCl_3$ δ (ppm); 7.375-7.258 (m, 9H, Biphenyl-CH), 7.098-7.016, m, 3H, C3, C4, C6-phenyl, 6.891-6.875 (t, 1H, J=8, C5-phenyl), 3.562 (s, 1H, NH) 3.419 (s, 1H, NH), 2.792 (s, 3H, CH3; 125 MHz- ^{13}C-NMR, Solvent-$CDCl_3$ δ: 166.356 (C=O), 152.754, 142.071, 141.879, 141.754, 139.086, 130.284, 130.140, 129.689, 129.410, 128.921, 128.633, 128.326, 127.155, 126.742, 126.425, 126.137, 113.429 (Aromatic carbons), 31.763 (methyl carbon); ESI-MASS (*m/z*): calculated- 318.38, found- 319.1 (M+1, 70%).

1-(4-phenoxyphenyl)-3-(m-tolyl)urea (14a)

Yield: 72%; MP: 152-154°C, IR (KBr, cm^{-1}): 3424 (N-H Stretch), 3097 (=C-H Stretch), 2994 (-C-H Stretch), 1739 (C=O Stretch-carbamide), 1599 (C=C Stretch); 500 MHz- ^{1}H-NMR, Solvent-$CDCl_3$ δ (ppm); 7.371-7.253 (m, 9H, Biphenyl-CH), 7.151-7.137 (m, 1H, J=8.5, C5-phenyl), 6.852-6.836 (m, 2H, J=8, C2, C4, C6-phenyl), 3.569 (s, 1H, NH), 3.496 (s, 1H, NH), 2.842 (s, 3H, CH_3); 125 MHz- ^{13}C-NMR, Solvent-$CDCl_3$ δ: 166.356 (C=O), 152.753, 142.102, 141.881, 141.754, 139.095, 130.285, 130.141, 129.691, 129.464, 128.936, 128.630, 128.321, 127.251, 126.447, 126.421, 126.034, 113.668 (Aromatic carbons), 33.510

(methyl carbon); ESI-MASS (*m/z)*: calculated- 318.38, found- 319.2 (M+1, 70%).

1-(4-phenoxyphenyl)-3-(p-tolyl)urea (15a)

Yield: 75%; MP: 156-158°C, IR (KBr, cm^{-1}): 3427 (N-H Stretch), 3095 (=C-H Stretch), 2994 (-C-H Stretch), 1740 (C=O Stretch-carbamide), 1587 (C=C Stretch); 500 MHz- ^{1}H-NMR, Solvent-$CDCl_3$ δ (ppm): 7.389-7.252 (m, 9H, Biphenyl-CH), 7.151-7.079 (dd, J=9, 1.6 Hz, 2H, C3-phenyl, C5-phenyl), 6.895-6.881 (d, J=8 Hz, 1H, C2, C6-phenyl), 4.645 (s, 1H, NH), 4.583 (s, 1H, NH), 2.979 (s, 3H-CH_3); 125 MHz- ^{13}C-NMR, Solvent-$CDCl_3$ δ: 166.317 (C=O), 149.059, 141.937, 141.678, 138.798, 129.353, 128.710, 128.489, 128.143, 127.932, 126.867, 126.329, 126.032, 125.868, 125.475, 124.390, 117.690, 113.803 (Aromatic carbons), 32.681 (methyl carbon); ESI-MASS (*m/z)*: calculated- 318.38, found- 319.4 (M+1, 75%);

Antitubercular screening

The Minimum Inhibitory Concentration (MIC) of the study compounds was evaluated against H37Rv strain of *Mycobacterium tuberculosis* by performing a Microplate Alamar-Blue assay (MABA).[13] The lowest concentration of the drug that prevented the growth of the Mtb was marked as the MIC. All the wells of 96 well plates were added with Middlebrook 7H9 broth media (100 µL) and the synthesized compounds were added at 100 to 0.2 µg/mL. All the wells except the blank well were then added with Mtb inoculum (100 µL). The parafilm wrapping was done and incubated at 37°C for continuous 5 days. The Alamar-blue reagent mixed with 10% tween 80 at a 1:1 ratio was added to each well (25 µL) and once again incubated for another twenty-four hours. The observation of pink colour in the well was recorded as the growth of the Mtb cells, whereas the blue colour was manifested as the absence of growth. The study was performed thrice to nullify the chance of error in interpretation.

Antibacterial screening

The antibacterial activity of the study compounds was performed against *E. coli* (ATCC 35218) and *S. aureus* (ATCC 25323) to understand the spectrum of activity exerted by the compounds. The Agar-plate disc-diffusion method was adopted for the study.[11,14] 20 mL of Mueller Hinton Agar was spread over the petri-dish. Then the inoculum of *E. coli* or *S. aureus* was prepared by mixing with sterile physiological saline solution by adjusting the turbidity to ~10^6 colony-forming units per millilitre. The prepared inoculum was then evenly streaked over the agar media in a petri dish. The synthesized compounds/ standards were saturated to Whatman paper discs of 6 mm diameter and positioned over the inoculated agar plate. Dimethyl sulfoxide was used as the negative control and Ciprofloxacin as the positive control. The treated agar plates were incubated for twenty-four hours. The lowest concentration of the drug that prevented the growth of the Mtb was recorded as the MIC against *S. aureus* and *E. coli*. The study was repeated thrice to obtain data in triplicate.

Cytotoxicity screening

The cytotoxicity of study compounds was evaluated against mammalian VERO cells to understand the safety of synthesized compounds against normal human cells. VERO Cells (1x 10^5 / well) were plated in 96-well plates containing 100µl of the medium and incubated in 5% CO_2 for twenty-four hours at 37°C. The cells were then incubated with test compounds at different concentrations (7.8 µg/mL to 1000 µg/mL) for another seventy-two hours. Samples were washed with pH 7.4 phosphate-buffered saline. MTT dye was introduced and once again incubated for four hours. DMSO (1mL) was added and absorbance was measured at 570nm to determine the percentage of cell viability.[15]

$$\% \text{ Cell Viability} = \frac{\text{Absorption recorded in test sample}}{\text{Absorption recorded in control}} \times 10$$

BBB permeability screening (PAMPA assay)

A membrane-permeability assay (PAMPA) was carried out to assess the Blood Brain Barrier (BBB) permeability of the study compounds.[16] The assay required an acceptor and a donor well plate. The acceptor plate was first moisturized with pH 7.4 buffer for 30 min. The buffer was then removed and the wells were coated with Porcine Brain Lipid (4 µL) having dodecane at 20 mg/mL concentration. The donor plate was transferred with 200 µL of test samples at 25 µg/mL concentration. BBB of Verapamil, Diazepam, Atenolol and Levofloxacin was performed for comparative study. Both the plates were then sandwiched and incubated for eighteen hours at room temperature. The sandwiched plates were then separated and recorded the absorbance in the acceptor plate as well as in the donor plate using an ELISA plate reader. The concentration of the drug that infused across the membrane was determined based on recorded absorbance by applying the following equation;

$$Pe\ (cm/s) = \{-\ln[1-CA(t)/Ceq]\}/[A*(1/VD+ 1/VA)*t]$$

Where, Pe is the measured permeability in cm sec^{-1}; A is filter area (i.e., 0.3 cm^2); VD is the volume of donor well (i.e 0.3 mL); VA is the volume of acceptor well (i.e., 0.2 mL); t is the duration of incubation (sec); CA(t) is the concentration of drug in acceptor well at particular time duration; CD(t) = concentration of drug in donor well at particular time duration.

$$Ceq = [CD(t)*VD + CA(t)*VA]/(VD+VA)$$

RESULTS AND DISCUSSION

Chemistry

As shown in Figure 2, the molecules were synthesized. It involved the synthesis of 1-bromo-4-phenoxy benzene (2) followed by 1-(4-phenoxy phenyl) urea (3). Different chlorobenzenes were reacted with 1-(4-phenoxyphenyl) urea to obtain the final derivatives. Concomitantly TLC was performed to monitor the progress/completion of the reaction. Crude products obtained at the end of the reaction were purified by performing column chromatography to get pure components. The final pure compounds were obtained with yields ranging from 45 to 79%. Melting point and TLC were performed to confirm the purity. ^{1}H and ^{13}C NMR and Mass Spectral data were obtained and structures of the synthesized compounds were interpreted.[16,17]

Antitubercular Activity

The antitubercular activity was determined by performing Micro Plate Alamar-Blue Assay on the synthesized compounds against the virulent strains of Mtb H37Rv.[13] Minimum Inhibitory Concentration (MIC) was calculated based on the presence or absence of the growth of Mtb and the result was recorded in Table 1. The structures of the study compounds were related to the anti-tubercular activity and found that the compounds containing nitro groups (3a, 7a) were found most active among all the compounds screened for antitubercular activity at MIC of 3.13µg/mL. The anti-tubercular activity of lead compounds 3a and 7a was found comparable to the standard Pyrazinamide (PYZ). Compounds containing the carboxylic group (8a, 9a) produced antitubercular activity at MIC of 6.25µg/mL. The electron-withdrawing nitro and carboxylic groups would have positively influenced the antitubercular activity. Further, the compounds containing the electron-donating methyl group (13a, 14a, 15a) have shown a drastic reduction in antitubercular activity. Varying the substitutions on the phenyl ring showed diverse results based on the nature of the substituent groups, while the basic core moiety (1a) retained the activity at MIC of 6.25µg/mL. It can be inferred that molecules designed in analogy to the parent molecule GSK 2556286 were found to exhibit a positive effect against *Mycobacterium tuberculosis* and they shall be further optimized for improved activity.

Antibacterial Activity

The synthesized compounds were further evaluated against *E. coli* and *S. aureus* to determine the spectrum of activity. The study was performed through the disc diffusion method.[18] Compounds 3a, 7a, 8a, and 9a have shown good activity against *S. aureus* at the concentration of 0.98 µg/mL in comparison to the standard Ciprofloxacin (CPFX) whereas against *E. coli*, compounds 2a, 3a, 7a-12a have produced activity only the concentration of 7.81µg/mL (Table 1). The compounds have shown comparatively better against *S. aureus* than *E. coli.* The difference in the activity between the gram-positive and gram-negative organisms may be related to the permeability of the molecules through the cell wall.[19] Compounds containing nitro and carboxylic groups were found to show better activity over other substituents against both *E. coli* and *S. aureus.*

Table 1: Antibacterial and Anti-tubercular effects of the study compounds.

Code	*S. aureus* MIC in µg/mL	*E. coli* MIC in µg/mL	Mtb MIC in µg/mL
1a	3.91	15.63	12.5
2a	1.95	7.81	6.25
3a	0.98	7.81	3.13
4a	3.91	15.63	>25
5a	3.91	15.63	12.5
6a	3.91	15.63	12.5
7a	0.98	7.81	3.13
8a	0.98	7.81	6.25
9a	0.98	7.81	6.25
10a	3.91	7.81	12.5
11a	1.95	7.81	12.5
12a	1.95	7.81	12.5
13a	15.63	31.25	>25
14a	15.63	31.25	>25
15a	15.63	31.25	>25
CPFX	1.95	3.91	3.13
PZA	Not Determined	Not Determined	3.13

Table 2: Cytotoxicity and selectivity index of the study compounds.

Code	CC_{50} in µg/mL [a]	Selectivity Index [b]
1a	255.5±0.64	20.4
2a	198.1±0.82	31.7
3a	190.3±0.37	60.8
4a	225.8±4.54	9.0
5a	232.4±0.83	18.6
6a	195.7±0.43	15.7
7a	190.2±0.66	60.8
8a	209.8±1.26	33.6
9a	220.4±0.83	35.3
10a	225.8±1.21	18.1
11a	222.5±2.55	17.8
12a	218.1±1.49	17.4
13a	232.8±0.81	9.3
14a	240.2±0.43	9.6
15a	244.2±0.45	9.8

[a] Data are provided as mean ± SEM (n =3)[b] Selectivity index- calculated by taking ratio of cytotoxicity (CC_{50}) to Mtb MIC

Table 3: Effective BBB permeability estimation of the study compounds.

Compound Code	P_e x10^{-6} cm/s	Classification
Verapamil (Peripheral drug)	0.0	Low permeability (CNS-)
Diazepam (CNS drug)	12.4	High permeability (CNS+)
Levofloxacin (Peripheral drug)	0.0	Low permeability (CNS-)
1a	2.3	Permeability Uncertain (CNS+/-)
2a	2.2	
3a	2.1	
4a	2.5	
5a	2.2	
6a	2.1	
7a	2.0	
8a	2.6	
9a	2.6	
10a	2.6	
11a	2.6	
12a	2.6	
13a	3.0	
14a	3.2	
15a	3.0	

Cytotoxicity Screening and Selectivity index

For a drug to be safe, it should not produce any toxicity towards normal cells. To evaluate the cytotoxicity, the study compounds were screened against the kidney epithelial cell line of an African green monkey. The concentration required to produce 50% cytotoxicity (CC_{50}) was determined and all the compounds exhibited CC_{50} >180 µg/mL, which falls in the safe range and proved the study compounds are non-toxic towards normal mammalian cells (Table 2). The selectivity of the molecules towards the desired activity will avoid the undesired side effects. The antitubercular drugs should show selectivity towards *Mycobacterium tuberculosis* rather than normal human cells. Therefore, the selectivity index of the synthesized compounds was calculated by taking the ratio of the obtained cytotoxicity (CC_{50}) values and the obtained antitubercular MIC values. The lead compounds from the anti-tubercular study (3a to 7a) showed a good selectivity index > 57 and the result of the compounds showed nominal selectivity >9. The lead compounds are selective towards Mtb and safe towards normal mammalian cells.

Blood Brain Barrier (BBB) Permeability

BBB permeability is the main cause for neurotoxicity of any peripherally acting drugs, therefore PAMPA assay needs to be performed to study the BBB permeability. The study provides important information about CNS+/- effects of the synthesized compounds. The BBB permeability of our study compounds was equated with drugs in the market and our compounds are classified into three categories viz low permeable (CNS-) having Pe= < 2.0 * 10^{-6} cm s^{-1}, high permeable (CNS+) having Pe= > 4.0 * 10^{-6} cm s^{-1}, and permeable uncertain (CNS+/-) having Pe =4.0 - 2.0 *10^{-6} cm s^{-1}. Diazepam is a highly permeable drug with Pe=12.4 x10^{-6} cm/s, whereas levofloxacin and verapamil are low permeable drugs with Pe=0.0 cm/s. The lead compounds of anti-tubercular study (3a and 7a) produced Pe of 2.1 * 10^{-6} cm s^{-1} and 2.0 * 10^{-6} cm s^{-1} respectively and classified under permeable uncertain (CNS+/-) (Table 3). The positive point is that the Pe is close to the border to be classified as low permeable (CNS-). Therefore, the lead compounds can be easily optimized to get into the low permeable (CNS-) class by introducing more polar groups as substituents in the phenyl ring.

Molecular Docking

The synthesized molecules were docked against HsaA monooxygenase (PDB ID: 3AFF) using a web-based molecular docking program 1-Click Mcule.[20] All the molecules entered the binding site of the substrate[21] and produced critical interactions with the active site residues Trp84, Ile88, Tyr120, Trp141, Ser143, Trp182, Leu187 and His368, which are presented in Table 4. The molecules 3a and 7a produced interaction/binding energies of -9.2 and -9.3 kcal/mol respectively, which are close to -10.1 kcal/mol of the parent molecule GSK 2556286. The docking poses of 3a and GSK 2556286 are shown in Figure 3. The molecules 2a, 8a

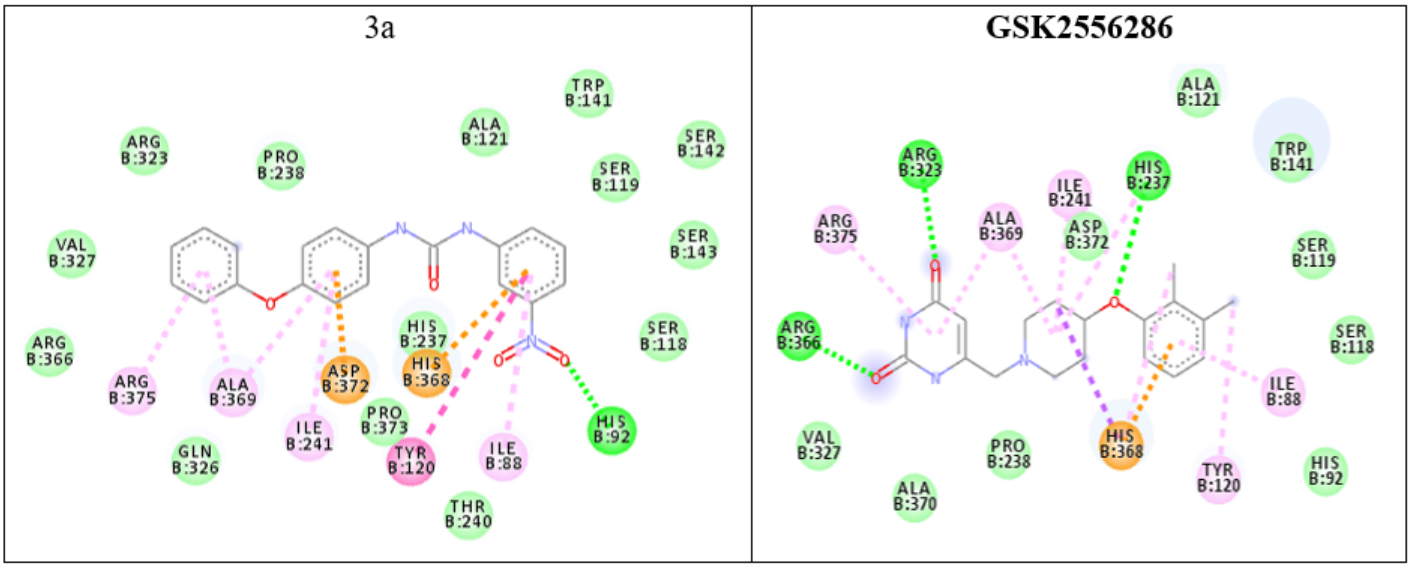

Figure 3: Docking poses of 3a and GSK 2556286 against HsaA monooxygenase.

Table 4: Binding energies and the interacting residues of HsaA monooxygenase with the ligand molecules.

Code	Binding/ Interaction energy (Kcal/mol)	Interacting residues of HsaA monooxygenase with the ligand molecules (Active site residues Trp84, Ile88, Tyr120, Trp141, Ser143, Trp182, Leu187 and His368)
1a	-7.5	His368, Ile88
2a	-8.8	His368, Ile88
3a	-9.2	His368, Ile88, Tyr120
4a	-7.3	His368, Ile88
5a	-7.5	His368, Ile88
6a	-7.3	His368, Ile88
7a	-9.3	His368, Ile88, Tyr120
8a	-7.8	His368, Ile88
9a	-7.9	His368, Ile88
10a	-6.9	His368, Tyr120
11a	-6.7	His368, Tyr120
12a	-6.0	His368, Tyr120
13a	-5.9	His368, Tyr120
14a	-5.8	His368, Tyr120
15a	-5.1	His368, Tyr120
GSK 2556286	-10.1	His368, Ile88, Tyr120

and 9a produced binding energies at -8.8 -7.8 and -7.9 Kcal/mol respectively, while the rest of the molecules produced binding energies below -7.5 kcal/mol. The results of the docking study proved apparent that there could be a correlation between the inhibition of HsaA monooxygenase and antitubercular activity. The parent molecule GSK 2556286 produced a docking score of -10.1 kcal/mol which is better than our study molecules. This indicates that GSK 2556286 could produce a better affinity towards the target HsaA monooxygenase. The study molecules must be further optimized for even better affinity towards the target.

CONCLUSION

A series of fifteen molecules were designed with drug-likeness using GSK 2556286 as the template molecule. They were then synthesized and evaluated for anti-tubercular activity and found compounds 3a and 7a were found to be effective and comparable to the standard drug Pyrazinamide. The same compounds were also proved to be effective against both gram-positive and gram-negative bacterial strains. Moreover, the lead compounds produced only negligible toxicity against the mammalian cell and exhibited reduced BBB permeability. The docking study had shown a correlation with the antitubercular activity, therefore it is postulated that the effective antitubercular activity from the lead compounds would have resulted from the novel mechanism of inhibiting HsaA monooxygenase involved in cholesterol metabolism. TB Alliance is working with GlaxoSmithKline, Bill and Melinda Gates Foundation and TB Drug Accelerator groups in developing a novel drug (GSK2556286) acting through a new mechanism. Contemporary to the research happening at the industry level, we attempted to develop such drug candidates at the academic institutional level. We believe that the lead molecules obtained from our study could provide a new vista for further drug discovery research against TB.

ACKNOWLEDGEMENT

The authors acknowledge the financial support from Karpagam College of Pharmacy for the purchase of the required chemicals for the study.

CONFLICT OF INTEREST

The authors declare that there is no conflict of interest.

REFERENCES

1. Chakaya J, Khan M, Ntoumi F, Aklillu E, Fatima R, Mwaba P, *et al*. Global *tuberculosis* Report 2020 – Reflections on the Global TB burden, treatment and prevention efforts. Int J Infect Dis. 2021;113(Suppl 1):S7-S12. doi: 10.1016/j.ijid.2021.02.107, PMID 33716195.
2. Gandhi NR, Nunn P, Dheda K, Schaaf HS, Zignol M, Van Soolingen D, *et al*. Multidrug-resistant and extensively drug-resistant *tuberculosis*: A threat to global control of tuberculosis. Lancet. 2010;375(9728):1830-43. doi: 10.1016/S0140-6736(10)60410-2, PMID 20488523.
3. World health organization. Global *tuberculosis* report 2021: Supplementary material. 2022.
4. Anderson RM, May RM. Directly transmitted infections diseases: Control by vaccination. Science. 1982;215(4536):1053-60. doi: 10.1126/science.7063839, PMID 7063839.
5. Palmer CE, Long MW. Effects of infection with atypical mycobacteria on BCG vaccination and *tuberculosis*. Am Rev Respir Dis. 1966;94(4):553-68. doi: 10.1164/arrd.1966.94.4.553, PMID 5924215.
6. Andersen P, Doherty TM. The success and failure of BCG - implications for a novel *tuberculosis* vaccine. Nat Rev Microbiol. 2005;3(8):656-62. doi: 10.1038/nrmicro1211, PMID 16012514.
7. Igarashi M, Ishizaki Y, Takahashi Y. New antituberculous drugs derived from natural products: Current perspectives and issues in antituberculous drug development. J Antibiot. 2017;71(1):15-25. doi: 10.1038/ja.2017.126, PMID 29089593.
8. Deb U, Biswas S. Pretomanid: The latest USFDA-approved anti-tuberculosis drug. Indian J Tuberc. 2021;68(2):287-91. doi: 10.1016/j.ijtb.2020.09.003. PMID 33845969.
9. Nuermberger EL, Martínez-Martínez MS, Sanz O, Urones B, Esquivias J, Soni H, *et al*. GSK2556286 is a novel antitubercular drug candidate effective *in vivo* with the potential to shorten *tuberculosis* treatment. Antimicrob Agents Chemother. 2022;66(6):e0013222. doi: 10.1128/aac.00132-22, PMID 35607978.
10. Suter CM. Synthesis in the diphenyl ether series. I. Preparation of some simple derivatives 1. J Am Chem Soc. 1929;51(8):2581-5. doi: 10.1021/ja01383a045.
11. Sellamuthu S, Asseri AH, Goojani HG, Nath G, Singh SK. Preliminary studies on ligand-based design and evaluation of new mycobacterial ATP synthase inhibitors. Curr Drug Ther. 2018;13(1):56-73. doi: 10.2174/1574885512666170911144732.
12. Sellamuthu S, Bhat MF, Kumar A, Nath G, Singh SK. Design, synthesis and biological evaluation of carbazole derivatives as antitubercular and antibacterial agents. Curr Bioact Compd. 2019;15(1):83-97. doi: 10.2174/1573407214666180226125501.
13. Lourenço MCS, De Souza MVNd, Pinheiro AC, Ferreira MdL, Gonçalves RSB, Nogueira TCM, *et al*. Evaluation of anti-tubercular activity of nicotinic and isoniazid analogues. Arkivoc. 2007(15):181-91. doi: 10.3998/ark.5550190.0008.f18.
14. Singh M, Kumar Singh S, Gangwar M, Sellamuthu S, Nath G, K. Singh S. Design, Synthesis and Mode of Action of Some New 2-(4';-aminophenyl) benzothiazole Derivatives as Potent Antimicrobial Agents. Lett Drug Des Discov. 2016;13(5):429-37. doi: 10.2174/1570180812666150821003220.
15. Mosmann T. Rapid colorimetric assay for cellular growth and survival: Application to proliferation and cytotoxicity assays. J Immunol Methods. 1983;65(1-2):55-63. doi: 10.1016/0022-1759(83)90303-4, PMID 6606682.
16. Di L, Kerns EH, Fan K, McConnell OJ, Carter GT. High throughput artificial membrane permeability assay for blood–brain barrier. Eur J Med Chem. 2003;38(3):223-32. doi: 10.1016/s0223-5234(03)00012-6, PMID 12667689.
17. Silverstein RM, Bassler GC. Spectrometric identification of organic compounds. J Chem Educ. 1962;39(11):546. doi: 10.1021/ed039p546.
18. Bharti SK, Nath G, Tilak R, Singh SK. Synthesis, anti-bacterial and anti-fungal activities of some novel Schiff bases containing 2,4-disubstituted thiazole ring. Eur J Med Chem. 2010;45(2):651-60. doi: 10.1016/j.ejmech.2009.11.008, PMID 19932927.
19. Silhavy TJ, Kahne D, Walker S. The bacterial cell envelope. Cold Spring Harb Perspect Biol. 2010;2(5):a000414. doi: 10.1101/cshperspect.a000414, PMID 20452953.
20. Vicidomini C, Roviello V, Roviello GN. *In silico* investigation on the interaction of chiral phytochemicals from *Opuntia ficus-indica* with SARS-CoV-2 Mpro. Symmetry. 2021;13(6):1041. doi: 10.3390/sym13061041.
21. Dresen C, Lin LY-C, D'Angelo I, Tocheva EI, Strynadka N, Eltis LD. A flavin-dependent monooxygenase from *Mycobacterium tuberculosis* involved in cholesterol catabolism. J Biol Chem. 2010;285(29):22264-75. doi: 10.1074/jbc.M109.099028, PMID 20448045.

Cite this article: Sellamuthu S, Sellapan M, Kandasamy CS, Kumar D, Kasimayan K, Manickavasagam S. Analog-based Design and Development of Novel Molecules as Anti-tubercular agents. Indian J of Pharmaceutical Education and Research. 2023;57(1s):s105-s113.